International Biodeterioration & Biodegradation 67 (2012) 28–39

Contents lists available at SciVerse ScienceDirect

International Biodeterioration & Biodegradation

journal homepage: www.elsevier.com/locate/ibiod

Interpretation of redox potential variation during biological denitrification using linear non-equilibrium thermodynamic model

Hong-Bang Cheng, Mathava Kumar, Jih-Gaw Lin*

Institute of Environmental Engineering, National Chiao Tung University, Hsinchu City 300, Taiwan

ARTICLE INFO

Article history:
Received 11 August 2011
Received in revised form
16 November 2011
Accepted 20 November 2011
Available online 21 December 2011

Keywords:
Affinity
Biological denitrification
Linear nonequilibrium thermodynamics
MIRROR model No. 1
ORP

ABSTRACT

In this study, the oxidation reduction potential (ORP) of biological denitrification processes is interpreted based on the MIRROR model No. 1, a linear non-equilibrium thermodynamic model developed in an earlier study. The model interconnects the affinities of catabolism and anabolism, the driving forces of microbial metabolism, with the system ORP and reaction rates of biological processes. Experimental results reported in the literature were used for calibrating the MIRROR model No. 1 to determine the optimal values of model stoichiometric, kinetic, and phenomenological parameters; the calibrated model was then used to simulate laboratory data. The simulation results agree well with the experimental observations. There is a close relationship between the affinities of catabolism and the system ORP of the biological denitrification process, but the ORP variation per unit affinity of catabolism is not a constant but proportional to the molarity of electrons transferred catabolically. The linear relationship between redox potential and reaction rate, which is derived based on MIRROR model No. 1, is subsequently verified by the experimental results reported in the literature. This linear relationship enables evaluation of the biological denitrification rate based on the real-time monitoring of the system ORP.

1. Introduction

During biological denitrification processes, electrons extracted from the carbon-hydrogen bonds of extracellular carbon are transferred to an electron transport chain. As the electrons travel down the transport chain, some of the energy released from the electrons is stored as high-energy phosphate bonds of ATP inside the microbial cells. Eventually, electrons are removed from the transport molecule to an acceptor, such as nitrate (NO_3^-), nitrite (NO_2^-), nitric oxide (NO) and nitrous oxide (N_2O). The electron transfer and the tendency of denitrification reactions can be monitored by using a sensitive and representative oxidation reduction potential (ORP) (Balakireva et al., 1974; Kjaergaard, 1977). For batch operations of biological denitrification processes under suitable conditions, the ORP curve shows an obvious bending point, also known as the knee point, that can be used to indicate the completion of biological denitrification reactions (Paul et al., 1998). Therefore, ORP has been widely used to monitor and control denitrification processes (Plisson-Saune et al., 1996).

Under equilibrium conditions, the modified-Nernst equation had been widely used to describe the relationship between the system ORP and the concentrations of reduced and oxidized species involved in denitrification processes. Chang et al. (2004) developed the modified-Nernst equation based on actual stoichiometric chemical equations for biological denitrification processes as shown in Eq. (1).

$$E_e = a'' + b''pH + c''\log\left(\left[NO_3^-\right]\right) \quad (1)$$

where E_e is electrode potentials (V) under equilibrium conditions; a'', b'' and c'' are constants. The Nernst equation can be used to depict the thermodynamically stable state, and describes the direction and extent of biological processes (Stumm and Morgan, 1996). However, it is usually limited to modeling dynamic variation of redox potential because of the equilibrium hypothesis (Stumm, 1966). In biochemical reactions, microorganisms always exchange substance and energy with their surrounding environment by diffusion or convection; therefore, true equilibrium conditions are rarely reached. In some instances, the theoretical ORP values calculated using the modified-Nernst equation is somewhat deviated from the experimental observations (Nagpal et al., 2000).

To overcome the defect of the Nernst equation, Cheng et al. (2007) developed a new ORP model called the microbial related reduction–oxidation reaction (MIRROR) model No. 1 based on linear non-equilibrium thermodynamics (NET). The model is composed of three major equations (Eqs. (2)–(4)):

* Corresponding author. Tel.: +886 3 5722681; fax: +886 3 5725958.
E-mail address: jglin@mail.nctu.edu.tw (J.-G. Lin).

0964-8305/$ – see front matter © 2011 Elsevier Ltd. All rights reserved.
doi:10.1016/j.ibiod.2011.11.010

$$\eta = E_{ne} - E_e = P_{EC}A_{BS}^{C} + P_{EA}A_{BS}^{A} \quad (2)$$

$$J_C = P_{CC}A_{BS}^{C} + P_{CA}A_{BS}^{A} \quad (3)$$

$$J_A = P_{AC}A_{BS}^{C} + P_{AA}A_{BS}^{A} \quad (4)$$

where η is overpotential, E_{ne} is electrode potentials (V) under non-equilibrium; J_C and J_A are the reaction rates of catabolism (C-mol g^{-1} h^{-1}) and anabolism (C-mol g^{-1} h^{-1}), respectively; A_{BS}^{C} and A_{BS}^{A} indicate affinities (J mol^{-1}) of catabolism (C) and anabolism (A), respectively, occurring in bulk solution (BS); and P_{ij} (i, j = E, C and A) are phenomenological parameters with E that represents the electrode process.

The phenomenological derivation of constitutive relations for fluxes within the framework of linear NET leads to the observation that the entropy production in biological systems can be viewed as a product of a driving force (affinity) and a flux (reaction rate). In MIRROR model No. 1, microbial metabolism is considered as a simple configuration that combines catabolism and anabolism. The energy needed to drive anabolic reactions is furnished by catabolism reactions, and coupling of energy-consuming reactions and corresponding electron-releasing reactions is quantified through phenomenological parameters of P_{CC}, P_{CA}, P_{AC} and P_{AA}. In addition, coupling of the ORP electrode processes to biological catabolism and anabolism are depicted by P_{EC} and P_{EA}, respectively. Biophysical models based on kinetic equations and equilibrium conditions fail to depict such coupling relationship satisfactorily; the concept of coupling is a unique characteristic of MIRROR model No. 1, but is not addressed in Eq. (1).

The affinities of catabolism and anabolism drive microbial metabolism to proceed, and the spontaneous reactions only proceed in the direction from higher affinities to low affinities. When the affinity of a reaction becomes zero, the reaction reaches an equilibrium condition (Demirel and Sandler, 2004). In Eq. (2), when both catabolism and anabolism affinities are zero, or η (i.e. $E_{ne} - E_e) = 0$, E_{ne} is equal to E_e (Cheng et al., 2007), both MIRROR model No. 1 and the Nernst equation have identical results. However, the MIRROR model No. 1 provides a more general description of system ORP than the Nernst equation for biochemical reactions under either equilibrium or non-equilibrium conditions.

One of the important presumptions of the MIRROR model No. 1 is that both ORP and reaction rates of microbial metabolism are linear functions of the affinities of catabolism and anabolism. Experimental and theoretical studies have shown that there exists a near-linear region of the relationship between the affinity and the biochemical reaction rate when the reaction approaches an equilibrium condition (Rottenberg, 1973; van der Meer et al., 1980). Moreover, the linearity is often observed between steady-state flows and conjugate thermodynamic forces outside the range of equilibrium for a number of biological systems even though the driving forces are expected to lead to considerable nonlinearity (Rothschild et al., 1980). However, the linear relationship between affinity and ORP (Eq. (2)) has not been applied for microbial systems. In this paper, this linear relationship is verified by simulating ORP variations of several biological denitrification processes reported in literatures using the MIRROR model No. 1. The simulation results are compared with the simulated results using the modified-Nernst equation (Eq. (1)) as proposed by Chang et al. (2004). The implication of phenomenological parameters has also been explained based on the electron flow during biological denitrification processes. Finally, properties and restrictions of the MIRROR model No. 1 to monitor and control biological denitrification processes are also discussed.

2. Methodology

The experimental data of several biological denitrification processes reported in the literature (Gao et al., 2011; Guo et al., 2007; Han et al., 2007; Yang et al., 2007; Yuan and Gao, 2010; Zhang et al., 2006) were collected for the present simulation studies. In the simulation process, biochemical reactions other than denitrification occurring at the electrode surface and the electrons accepted are neglected (Stumm and Morgan, 1996). Initially, the ORP data were simulated using the modified-Nernst equation by conducting multiple linear regression analyses with the simple least squares as the subjective function (Chang et al., 2004); ORP was used as a dependent variable whereas the pH and log($[NO_3^-]$) were treated as independent variables.

Protocols for simulating the biological denitrification data using MIRROR model No .1, and evaluating the model performance are listed in Table 1. Detailed procedures of these stepwise protocols are discussed below.

2.1. Calculation of affinities

For a redox reaction, the affinity can be calculated using Eq. (5) (Nielsen, 1997).

$$A_{BS}^{m} = -\Delta G_m^0 - RT\ln\left(\prod X^S\right), \quad m = C \text{ or } A \quad (5)$$

where, ΔG_m^0 is the change in standard Gibbs free energy of catabolism or anabolism; R is gas constant (8.314 J mol^{-1} K^{-1}); T is temperature (K); S is the stoichiometric coefficient (positive for products and negative for reactants); and X is the molar concentration of redox species. The carbon unit has to be converted from mg $CODL^{-1}$ into molar concentration by the degree of reduction balance (Heijnen, 1999). Values of Gibbs free energies excluding biomass are excerpted from the data published by Rittmann and McCarty (2001) whereas the Gibbs free energy of biomass computed by Xiao and VanBriesen (2008) was used for calculating the change in Gibbs free energy of anabolism. Acquisition of the generalized stoichiometric coefficients and data for the biological denitrification processes in question is discussed below.

Table 1
Stepwise protocol followed for the simulation of biological denitrification data using MIRROR model No. 1.

Step	Protocol
Calculating the affinities of catabolism and anabolism	Calculating the affinities of catabolism and anabolism by corresponding stoichiometric parameter and reactant concentration. 1. Obtain stoichiometric equation. i. Identification of generalized biological denitrification reaction ii. Estimation of f_e, f_s, $f_{NO_2^-}$ and $f_{NO_3^-}$ iii. Obtain stoichiometric equation of catabolism and anabolism by generalized biological denitrification reaction. 2. Obtain concentration of reactants. i. Digitalization of the experimental data of biological denitrification process collected from various published papers, including pH, ORP, COD, NH_4^+, NO_2^- and NO_3^- ii. Calculate the concentration of N_2, CO_2 and HCO_3^-.
Parameter estimation	Analysis of phenomenological parameters P_{EC} and P_{EA} by the multiple linear regressions.
Performance evaluation	R^2, simultaneous F test of unit slope and zero intercept, Lilliefor's test, EF, Deviance measures (RMSE) and model discrimination.

2.1.1. General stoichiometric equation for biological denitrification processes

Nitrate and nitrite are used as electron acceptors for the biological denitrification processes; nitrate can be converted into molecular nitrogen via several reaction steps, including (1) the conversion of nitrate ions to nitrite ions, (2) the conversion of nitrite ions to nitric oxide, (3) the conversion of nitric oxide to nitrous oxide, and (4) the conversion of nitrous oxide to molecular nitrogen. Nitric oxide and nitrous oxide are considered to be the intermediates so that they are not included in the model. The stoichiometric coefficients and the generalized catabolic and anabolic equations of biological denitrification reactions have been deduced according to the methods presented by Rittmann and McCarty (2001). The overall stoichiometric equation of electron transfer for biological denitrification includes half reactions of nitrate and nitrite reduction, shown as Eqs. (6) and (7), respectively.

$$\frac{1}{2}NO_3^- + \frac{1}{2}H_2O + e^- \rightarrow \frac{1}{2}NO_2^- + OH^- \quad (6)$$

$$\frac{1}{3}NO_2^- + \frac{2}{3}H_2O + e^- \rightarrow \frac{1}{6}N_2 + \frac{4}{3}OH^- \quad (7)$$

The overall reaction of electron acceptor was obtained by combining Eqs. (6) and (7) into Eq. (8)

$$\frac{1}{2}f_{NO_3^-}NO_3^- + \left(\frac{1}{3}f_{NO_2^-} - \frac{1}{2}f_{NO_3^-}\right)NO_2^- + \left(\frac{1}{2}f_{NO_3^-} + \frac{2}{3}f_{NO_2^-}\right)H_2O + e^- \rightarrow \frac{1}{6}f_{NO_2^-}N_2 + \left(f_{NO_3^-} + \frac{4}{3}f_{NO_2^-}\right)OH^- \quad (8)$$

where $f_{NO_3^-}$, and $f_{NO_2^-}$ are fractions of electrons accepted during nitrate and nitrite reduction reaction, respectively; summation of $f_{NO_3^-}$ and $f_{NO_2^-}$ is equal to 1. $f_{NO_3^-}$ and $f_{NO_2^-}$ can be calculated by using Eq. (9) and Eq. (10), respectively.

$$f_{NO_3^-} = \frac{2\Delta\left[NO_3^-\right]}{5\Delta\left[NO_3^-\right] + 3\Delta\left[NO_2^-\right]} \quad (9)$$

$$f_{NO_2^-} = \frac{3\Delta\left[NO_3^-\right] + 3\Delta\left[NO_2^-\right]}{5\Delta\left[NO_3^-\right] + 3\Delta\left[NO_2^-\right]} \quad (10)$$

Oxidation of organic compounds that are used as electron donors in heterotrophic biological denitrification reactions can be described using the oxidation reactions proposed by Rittmann and McCarty (2001) shown as Eq. (11). The organic matter is expressed in a general formula that may represent a variety of carbon sources:

$$\frac{1}{q}C_aH_bO_cN_d^{-n} + \frac{2a-c+d+n}{q}H_2O \rightarrow \frac{a-d-n}{q}CO_2 + \frac{d}{q}NH_4^+ + \frac{d+n}{q}HCO_3^- + H^+ + e^-q = 4a + b - 2c - 3d + n \quad (11)$$

The half reactions of nitrate and nitrite reduction cannot proceed spontaneously; they have to be combined with the other half reaction of organics oxidation (Eq. (11)) to form a complete equation, as shown in Eq. (12).

$$\frac{1}{2}f_{NO_3^-}NO_3^- + \left(\frac{1}{3}f_{NO_2^-} - \frac{1}{2}f_{NO_3^-}\right)NO_2^- + \frac{1}{q}C_aH_bO_cN_d^{-n} \rightarrow \frac{1}{6}f_{NO_2^-}N_2 + \left(1 - \frac{2a-c+d+n}{q} - \frac{1}{2}f_{NO_3^-} - \frac{2}{3}f_{NO_2^-}\right)H_2O + \frac{a-d-n}{q}CO_2 + \frac{d}{q}NH_4^+ + \frac{d+n}{q}HCO_3^- + \left(f_{NO_3^-} + \frac{4}{3}f_{NO_2^-} - 1\right)OH^- \quad (12)$$

Only a portion of available electrons in the organic compound is transferred to nitrate and nitrite during catabolic processes; hence, the overall catabolic equation for denitrification processes can be represented by Eq. (13), in which f_e is the fraction of total electron used for energy production.

$$\frac{1}{2}f_{NO_3^-}f_eNO_3^- + \left(\frac{1}{3}f_{NO_2^-}f_e - \frac{1}{2}f_{NO_3^-}f_e\right)NO_2^- + \frac{1}{q}f_eC_aH_bO_cN_d^{-n} \rightarrow \frac{1}{6}f_{NO_2^-}f_eN_2 + \left(f_e - \frac{2a-c+d+n}{q}f_e - \frac{1}{2}f_{NO_3^-}f_e - \frac{2}{3}f_{NO_2^-}f_e\right)H_2O + \frac{a-d-n}{q}f_eCO_2 + \frac{d}{q}f_eNH_4^+ + \frac{d+n}{q}f_eHCO_3^- + \left(f_{NO_3^-}f_e + \frac{4}{3}f_{NO_2^-}f_e - f_e\right)OH^- \quad (13)$$

Ammonium is assumed not to be the limited substrate in biological denitrification processes; it is the main nitrogen source of biomass. The half reaction of cell synthesis (assuming bacterial composition as $C_5H_7O_2N$) can be represented by Eq. (14).

$$\frac{1}{5}CO_2 + \frac{1}{20}NH_4^+ + \frac{1}{20}HCO_3^- + H^+ + e^- \rightarrow \frac{1}{20}C_5H_7O_2N + \frac{9}{20}H_2O \quad (14)$$

However, some electrons are transferred from carbon sources to microbial cells so that the organic compounds oxidizing half reaction can be represented by Eq. (11). The overall anabolic reaction for denitrification processes can further be obtained by combining Eqs. (11) and (14) to form Eq. (15).

$$\frac{1}{q}C_aH_bO_cN_d^{-n} + \left(\frac{1}{20} - \frac{d}{q}\right)NH_4^+ + \left(\frac{5}{4} - \frac{a}{q}\right)HCO_3^- \rightarrow \frac{1}{20}C_5H_7O_2N + \left(\frac{9}{20} - \frac{2a-c+d+n}{q}\right)H_2O + CO_2 + \left(\frac{6}{5} - \frac{a-d-n}{q}\right)OH^- \quad (15)$$

Because only a portion of the electrons contained in the carbon sources is needed for cell synthesis (whereas the rest is used for catabolism), the overall anabolic reaction can be obtained by multiplying Eq. (15) by the fraction of total electrons used for biomass synthesis (f_s) shown as Eq. (16).

$$\frac{1}{q}f_sC_aH_bO_cN_d^{-n} + \left(\frac{1}{20}f_s - \frac{d}{q}f_s\right)NH_4^+ + \left(\frac{5}{4}f_s - \frac{a}{q}f_s\right)HCO_3^- \rightarrow \frac{1}{20}f_sC_5H_7O_2N + \left(\frac{9}{20}f_s - \frac{2a-c+d+n}{q}f_s\right)H_2O + f_sCO_2 + \left(\frac{6}{5}f_s - \frac{a-d-n}{q}f_s\right)OH^- \quad (16)$$

Values of f_e and f_s can be obtained by applying the expanded thermodynamic model developed by Xiao and VanBriesen (2008).

2.1.2. Data collection and processing

Batch biological denitrification data including temperature, biomass, COD, ammonium, nitrite and nitrate, were excerpted from several published papers (Gao et al., 2011; Guo et al., 2007; Han et al., 2007; Yang et al., 2007; Yuan and Gao, 2010; Zhang et al., 2006). The data were digitized using GetData Graph Digitizer® 2.23; the reaction time was set to "zero" at the beginning of the experiment. The beginning and ending of each biological denitrification reaction were determined based on the bending points shown on both ORP and pH curves (Han et al., 2007), and the

variations of DO, ammonium, nitrite and nitrate curves. Concentrations of dissolved N_2 and CO_2 in the aqueous solution are estimated using Henry's law.

The simulation process assumes that biological denitrification processes proceed in aqueous solution with the water molar concentration being close to 1. The molar concentration of HCO_3^- at any time within the period of biological denitrification process can be calculated using Eq. (17), and the first dissociation constant of carbonic acid (K_1) is calculated using Eq. (18) (Chapra, 1997).

$$\left[HCO_3^-\right] = \frac{K_1}{\left[H^+\right]} K_H p_{CO_2} \tag{17}$$

$$K_1 = 10^{-(3404.71/T) - 0.032786T + 14.8435} \tag{18}$$

2.2. Estimation of phenomenological parameters

P_{EC} and P_{EA} were analyzed by using multiple linear regressions (MLR) with the simple least squares as the subjective function. MLR allows multiple independent variables to be simultaneously evaluated in the regression calculation (Tedeschi, 2006). The catabolism and anabolism affinities were selected as independent variables, and the non-equilibrium ORP was selected as dependent variable for estimating values of P_{EC} and P_{EA}. The MLR procedure is performed by using MINITAB 15 statistical software (Minitab Inc., PA, USA). Subsequently, the least mean squares analysis is carried out to minimize the mean squared error between the measured ORP and the calculated ORP using MIRROR model No. 1 for each sampling point.

2.3. Performance evaluation

Results of simulation using the MIRROR model No. 1 and modified-Nernst equation were compared with the experimental data obtained at each reaction time, and the differences were examined using several statistical validation procedures as listed in Tables 2 and 3. The deviance measurement method that includes the root mean square error (RMSE) was used for calculating the model bias (Mayer and Butler, 1993). The statistical significance of the bias was further tested by using the simultaneous F test of unit slope and zero intercept (F-test$_{s1,i0}$), which were obtained from the linear relation between the observed and predicted ORP after regression analyses (Mayer et al., 1994). The adjusted coefficient of determination (R^2) for the multiple linear regression between the simulated and experimental ORP data was used to evaluate the effectiveness of simulation. Besides, an overall indication of goodness-of-fit was evaluated based on the modeling efficiency (EF) (Confalonieri et al., 2010) as shown in Table 2.

Generally, a better simulation of a data set can be achieved with increasing number of parameters used in the model. However, the possibility that uncertainty of the parameter estimated also increases with more parameters is undesirable (Van Boekel, 2008). Therefore, comparing the MIRROR model No. 1 with the modified-Nernst equation only based on goodness-of-fit indices is not sufficient; a model discrimination method (Box and Hill, 1967) must also be used. This method discriminates the rival model based on the magnitude of residual sums of squares (RSS); a better model has a lower RSS value. The posterior probability to identify the best model is calculated as a function of the RSS.

The effect of DO and seeding sludge on the biological nitrogen removal process in a sequencing batch reactor (SBR) with suspensions of aerobic granular sludge has been investigated by Yuan and Gao (2010) and Gao et al. (2011). The SBR is operated sequentially in five phases, including (1) wastewater filling, (2) aerobic phase, (3) anoxic phase, (4) sludge settling, and (5) effluent discharge. In the study of Yuan and Gao (2010), DO concentrations in the SBR during the aerobic phase were controlled at four different levels (i.e. 4.5 mg L^{-1}, 3.5 mg L^{-1}, 2.5 mg L^{-1} and 1.0 mg L^{-1}). Except the initial DO concentration, other operating conditions in four different sets of reactors including quantities of seeding sludge and synthetic

Table 2
Statistical indices and test used for evaluating the performance of simulation results of MIRROR model No. 1 and Nernst equation (Box and Hill, 1967; Confalonieri et al., 2010; Dallal and Leland, 1986; Mayer and Butler, 1993; Mayer et al., 1994).

Methodology	Purpose	Detailed expression/formulae	Remarks
F-test for slope = 1 and intercept = 0 (F-test$_{s1,i0}$)	To evaluate the regression line of experimental versus simulation data plots	$F = \frac{N(b_0-0)^2 + 2\sum \hat{y}_i(b_0-0)(b_1-1) + \sum \hat{y}_i^2(b_1-1)^2}{2\sum(y_i-\hat{y}_i)^2/(N-2)}$ where N is the number of experimental data. b_0 is the intercept and b_1 is slope y_i is experimental data, $\hat{y}_i$ is simulation data and $\bar{y}_i$ is the predicted value from $y_i = b_0 + b_1\hat{y}_i$. The degrees of freedom are 2 and $n-2$ for the numerator and denominator, respectively.	For an acceptable model, the regression line of experimental versus simulation data plots will be a 45° line through the origin. The F-test$_{s1,i0}$ is used to evaluate the regression line by test whether the intercept is 0 and slope is 1 simultaneously.
Lilliefor's statistics	Testing the hypotheses of normal distribution of the regression residuals	$KS = \max_x \lvert SCDF(x) - CDF(x)\rvert$ where CDF is the normal cumulative distribution function with mean and standard deviation equal to the mean and standard deviation of the sample and SCDF is the estimated empirical cumulative distribution function based on the sample.	If maximum discrepancy between SCDF and CDF is statistically significant, rejection of the null hypothesis is thus required.
The root mean square error (RMSE)	Quantifying the deviance between experimental and simulation data	$RMSE = \sqrt{[\sum(y_i-\hat{y}_i)^2]/N}$	A perfect fit is indicated by either RMSE being zero.
The adjusted coefficient of determination (R^2)	Quantifying the proportion of variation explained by the fitted regression line	$R^2 = 1 - (SS \text{ about line of best fit})/(Corrected SS \text{ of } y_i)$ where SS is sum of squares.	R^2 close to 1 means the model can be explained the variations of experimental data well.
The modeling efficiency (EF)	Evaluation overall indication of goodness-of-fit	$EF = 1 - \frac{\sum(y_i-\hat{y}_i)^2}{\sum(y_i-\bar{y})^2}$ where $\bar{y}$ is average of experimental data.	The EF value close to 1 means that the model is a near-perfect model.
Model discrimination method	To discriminate the rival model with the residual sums of squares (RSS)	$P_i = R_i/\sum R_i$ where P_i is posterior probability of being the better model, R_i is equal to $(RSS_{min}/RSS_i)^{0.5(n-p)}$. The summation is over the rival models, and RSS_i is residual sum of squares of model i; RSS_{min} is the smallest residual sum of squares in the set of all rival models, and p is the number of estimated parameters in each model.	The better model has higher posterior probability.

Table 3
Calibrated phenomenological and kinetics parameters used to simulate the ORP variation by MIRROR model No. 1.

Literature	Zhang et al. (2006)	Case-Gu1 (Guo et al., 2007)	Case-Gu2 (Guo et al., 2007)	Han et al. (2007)	Yang et al. (2007)	Case-Y1 (Yuan and Gao, 2010)	Case-Ga1 (Gao et al., 2011)
Carbon source	Acetic acid	Ethanol	Ethanol	Acetic acid	Ethanol	Glucose	Glucose
MIRROR model No. 1							
f_e	0.72	0.61	0.61	0.72	0.61	0.64	0.64
f_s	0.28	0.39	0.39	0.28	0.39	0.36	0.36
$f_{NO_3^-}$	0.37	0.33	0.24	0.38	0.026	0.022	0.032
$f_{NO_2^-}$	0.63	0.67	0.76	0.62	0.97	0.98	0.97
K_1 (M)	4.71×10^{-7}	4.71×10^{-7}	4.71×10^{-7}	4.21×10^{-7}	4.71×10^{-7}	4.76×10^{-7}	4.76×10^{-7}
K_H (M atm^{-1})	3.01×10^{-2}	3.01×10^{-2}	3.01×10^{-2}	3.82×10^{-2}	3.02×10^{-2}	2.94×10^{-2}	2.94×10^{-2}
P_{EC} (mV mol J^{-1})	0.41	0.088	0.29	0.24	−0.050	0.092	0.14
P_{EA} (mV mol J^{-1})	0.0020	0.099	0.057	1.44	0.11	0.0067	−0.0094
E_e (mV)	−1509.19	−813.55	−1114.37	−3535.75	−495.79	−417.38	−530.24
Modified Nernst equation							
a''	2338.07	1901.85	2518.79	12905.81	1295.57	610.49	1244.97
b''	−248.52	−242.75	−294.29	−1519.25	−195.68	−77.11	−69.92
c''	138.15	27.28	87.56	105.76	−40.12	−2.05	177.49

wastewater were controlled at similar levels. Therefore, simulating the experimental data of different anoxic stages was suitable for verifying the generality of predictions and robustness of the MIRROR model No. 1. In this paper, the data obtained from three sets of studies with DO controlled at 4.5 mg L^{-1}, 3.5 mg L^{-1}, and 2.5 mg L^{-1} were digitalized and identified as case-Y1, case-Y2 and case-Y3, respectively. The data sets of case-Y2 and case-Y3 were simulated using the model that has been calibrated using the case-Y1 data set. The model performance was also evaluated by its capability of reproducing case-Y2 and case-Y3 results. In addition, aerobic granular sludge and flocculent activated sludge, which had been used by Gao et al. (2011) to characterize nitrogen removal via nitrite and other operation conditions of SBR, i.e. pH, inflow synthetic wastewater and temperature, were controlled at similar levels. The data of experimental set with aerobic granular sludge and flocculent activated sludge as the seeding sludge (Gao et al., 2011) were digitalized and named as case-Ga1 and case-Ga2. The data sets of case-Ga2 were simulated using the model calibrated with the case-Ga1 data set, and the model performance was further evaluated by using statistic indices. In this paper, residual analyses for evaluating linear multiple regression are also included. If the calibrated model is adequate for simulating the data, the residuals should show no obvious structural pattern. The Lilliefor's test was used to test the normality of the residuals (Dallal and Leland, 1986).

3. Results and discussion

3.1. Statistical evaluation of ORP simulation and model discrimination

The simulating results of MIRROR model No. 1 and the modified Nernst equation are listed in Table 4. Two data sets excerpted from the study of Guo et al. (2007) are digitized and identified as case-Gu1 and case-Gu2. The correlation between simulated data and experimental results are indicated by R^2 and EF values. R^2 values of MIRROR model No. 1 are distributed over a narrow range, and are the best for case-Gu1 data (Guo et al., 2007) and the data set reported by Yang et al. (2007) (0.99), and the worst for the data reported by Han et al. (2007) (0.92). All R^2 values for the modified-Nernst equation, except the data reported by Zhang et al. (2006), are lower than those for MIRROR model No. 1. The results of EF show similar trend as R^2; the data sets with higher R^2 have higher EF.

To indicate the position of the perfect fit, and any biases that may be present in certain sections or the overall data, the experimental ORP (ORP_{exp}) is plotted versus the simulated ORP (ORP_{sim}); the results are shown in Fig. 1 marked as $ORP_{exp} = ORP_{sim}$. If the simulated ORP values are close to the experimental results, the intercept and slope of the regression line will approach to 0 and 1, respectively. Moreover, the F-test$_{s1,i0}$ is also used to test whether the intercept of 0 and slope of 1 are simultaneous. According to Fig. 1(e) and (g), the simulated ORP values using either MIRROR model No. 1 or the modified-Nernst equation have a good fit of the data reported by Yang et al. (2007) and the case-Ga1 (Gao et al., 2011) as confirmed by the non-significance ($P < 0.05$) of the F-test$_{s1,i0}$. Similar variance of residuals can be observed for the simulation results of the MIRROR model No. 1 and modified-Nernst equation for the data reported by Zhang et al. (2006), case-Gu2 data set (Guo et al., 2007) and Han et al. (2007) (Fig. 1(a), (c) and (d)). The bias of the MIRROR model No. 1 and modified-Nernst equation occurs primarily at the lowest ORPs. Because the ORP decreases with progressing biological denitrification reactions, the bias occurs primarily at the end of the biological denitrification process. Although non-uniform distribution of residuals are observed for several cases, the bias is not significant for all of the simulation results of the MIRROR model No. 1 and modified-Nernst equation based on the results of F-test$_{s1,i0}$ (Table 4).

RMSE can be used to measure the deviance of simulation results using MIRROR model No. 1 and modified-Nernst equation. The RMSE values shown in Table 4 reveal that the MIRROR model No. 1 results have smaller RMSE than the modified Nernst equation results for all cases except the case of Zhang et al. (2006). However, the difference between the RMSE of the MIRROR model No. 1 and modified Nernst equation is quite small (only 0.05). The results indicate that MIRROR model No. 1 is capable of simulating the ORP data with considerable accuracy; thereby, this model can be recommended for simulating the ORP variation during biological denitrification processes. The RMSE of the MIRROR model No. 1 are related to the final ORP value for all carbon sources (Fig. 2). When the final ORP variations are between −80 to −160 mV, the RMSEs are maintained at 1.8 and 4, respectively. If the final ORP is lower than −160 mV, the RMSE increases sharply. As mentioned before, the biases occur mainly at the completion of biological processes during which the redox couple for the biological denitrification process is consumed completely. The occurrence of some other non-nitrogen biological processes such as biological sulfate reduction may slightly affect the ORP measurement (Han et al., 2008; Plisson-Saune et al., 1996).

The results of statistical indices and deviance measures suggest that MIRROR model No. 1 is equal to, i.e. in the case of Zhang et al.

Table 4
Statistical evaluation of the simulation performances of the MIRROR model No. 1 and modified-Nernst equation.

Statistical test and parameters	Simultaneous F test of unit slope and zero intercept, $F_{s1,i0}$	R^2	EF	RMSE	Posterior probability of model discrimination
Zhang et al. (2006)					
M	3.88***	0.94	0.97	2.48	0.49
N	3.88***	0.96	0.97	2.43	0.51
Case-Gu1 (Guo et al., 2007)					
M	3.47***	0.99	0.99	6.58	0.55
N	3.47***	0.99	0.99	6.78	0.45
Case-Gu2 (Guo et al., 2007)					
M	3.33***	0.95	0.95	12.04	0.77
N	3.25***	0.93	0.93	14.70	0.23
Han et al. (2007)					
M	2.91***	0.97	0.97	9.22	0.61
N	4.29***	0.96	0.96	10.10	0.39
Yang et al. (2007)					
M	2.98***	0.99	0.99	4.19	0.76
N	2.96***	0.99	0.99	5.30	0.24
Case-Y1 (Yuan and Gao, 2010)					
M	4.00***	1.00	1.00	1.82	0.75
N	3.96***	0.98	0.99	5.52	0.25
Case-Ga1 (Gao et al., 2011)					
M	3.96***	0.99	0.99	4.36	0.63
N	3.89***	0.98	0.97	7.49	0.37

M, the MIRROR model No. 1; N, the modified-Nernst equation. Significance level: ***$P < 0.05$.

(2006) and case-Gu1 data set (Guo et al., 2007), or better than the modified-Nernst equation for simulating ORP of biological denitrification processes. However, MIRROR model No. 1 has more parameters and hence higher uncertainty than the modified-Nernst equation. Therefore, the test for model discrimination is necessary for selecting the better one between the two models. The posterior probabilities of the two models are shown in Table 4. MIRROR model No. 1 is overwhelmingly favored based on model discrimination analyses for all cases except the case of Zhang et al. (2006). In the case-Gu1 data set (Guo et al., 2007), the computed posterior probabilities indicate a 77% probability for MIRROR model No. 1 and only 23% probability for the modified-Nernst equation to yield correct answers. For the case-Y1 data set (Yuan and Gao, 2010), MIRROR model No. 1 has the larger posterior probabilities because the simulated data are over-estimated by the modified-Nernst equation at lower ORPs. In the modified Nernst equation proposed by Chang et al. (2004), nitrate is assumed to be the major electron acceptor so that the variation of nitrite concentration can be ignored. However, the experimental conditions in the studies of Yuan and Gao (2010) does not conform to this assumption; the initial concentrations of nitrite and nitrate were 13.23 mg L^{-1} and 0.92 mg L^{-1}, respectively. Therefore, the simulated results of ORP obtained by using the modified Nernst equation cannot fit the real experimental data.

3.2. Mechanistic implications of the MIRROR model No. 1

The variation of ORP and affinities of catabolism and anabolism reported by Han et al. (2007) are shown in Fig. 3. According to linear NET, the input substrate flow converts to output biomass flow in the microbial system, and both flows are caused by conjugated forces (Demirel and Sandler, 2002). The thermodynamic force that conjugates to catabolism and anabolism is identical to the affinity (negative value of free energy change, $-\Delta G$) of catabolism and anabolism. As shown in Fig. 3 that both catabolism and anabolism affinities are positive, Eqs. (13) and (16) are expected to proceed toward right that coincides with the variation of reactants including COD, ammonium, nitrite and nitrate. In addition, affinities of catabolism and anabolism decrease during the biological denitrification reaction, which means that biological denitrifcation processes have the tendency to approach equilibrium. The main reason for this phenomenon is that the medium conserving chemical energy for microbial metabolism is not continuously introduced into the reactor until the next feeding stage.

In Fig. 3, the time-dependent variations of both affinities of catabolism and system ORPs are noted to consist of two stages. During the first stage (0 to 49 min), the affinities of catabolism decrease linearly with a slope of -2.08 J mol^{-1} min^{-1}, and during the second stage, the negative decreasing rates decreases to -6.65 J mol^{-1} min^{-1}. Similar trends are observed with the ORP time-dependent variation. The time corresponding to the crossing point of straight-line plots for these two stages is the same for the affinity of catabolism and ORP. However, the affinity of anabolism decreases almost continuously at constant rate for the entire reaction period. Therefore, ORP is mainly affected by the driving force of the catabolism but not the driving force of the anabolism process. The carbon source used during biological denitrification processes has contributed to these observations. The study of Han et al. (2007) show easily biodegradable organic compounds, e.g. acetate acid, are noted to be immediately consumed as a carbon source at the beginning of the denitrification process. The thermodynamic efficiency of growth is defined as "(output force) - × (output flux)/[(input force) × (input flux)]" (Demirel and Sandler, 2002), and it is closely related to the degree of reduction of the substrate used as energy sources (Westerhoff et al., 1983). The degree of reduction of an organic compound (γ_{COD}) can be defined as the number of electrons involved in its oxidation to CO_2, H_2O, and NH_3 (Duboc et al., 1995). For a compound with chemical formula $C_aH_bO_cN_d^{-n}$, and charge n, the degree of reduction that is defined by Eq. (19) to reflect the valence states of the four elements.

$$\gamma_{COD} = (4a + b - 2c - 3d + n)/a \tag{19}$$

When organic substrates with a similar degree of reduction as biomass (degree of reduction of biomass = 4.2), e.g. glucose, lactate or acetate, are used as carbon sources, the thermodynamic efficiency is almost zero with only a small portion of chemical energy liberated during catabolism and transferred to the biomass synthesis reaction (Westerhoff et al., 1983). Consequently, the affinity of anabolism in Fig. 3 only has an inappreciable interaction with the variation of ORP during biological denitrification processes.

The coupling phenomena between the electrode process and catabolism or anabolism can be quantified using the phenomenological parameters, P_{EC} and P_{EA}. Values of P_{EC} and P_{EA}, shown in Table 3, are in the range of -0.050 to 0.41 mV J^{-1} mol and -0.0094 to 1.44 mV J^{-1} mol, respectively. According to Eq. (2), the redox couple of both catabolism and anabolism in a bulk solution may contribute to ORP measurement. Therefore, the discussion of ORP has to include mixed potential (Peiffer et al., 1992) so that P_{EC} and P_{EA} can be interpreted as the overpotential change per unit affinity during catabolism and anabolism, respectively. Because the overpotential is always defined with respect to a specific reaction with known E_e (Gileadi, 1993), P_{EC} and P_{EA} can also be interpreted as ORP change per unit affinity during catabolism and anabolism, respectively. As mentioned before, the affinities of catabolism and anabolism are both positive during biological denitrification processes; hence, only signs of P_{EC} and P_{EA} are identical to the sign of

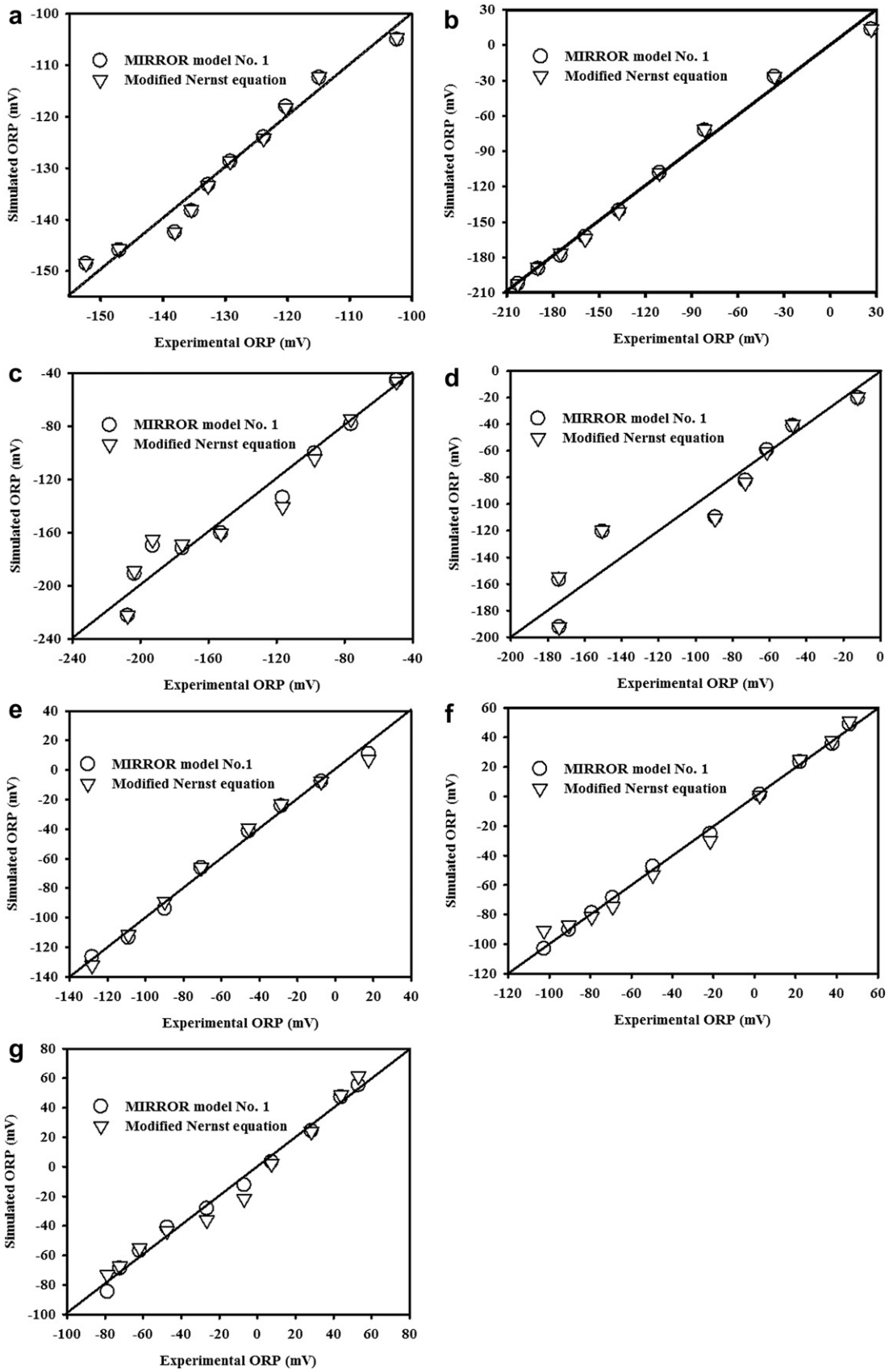

Fig. 1. Experimental versus simulation plot of literatures (a) Zhang et al. (2006), (b) case-Gu1 (Guo et al., 2007), (c) case-Gu2 (Guo et al., 2007), (d) Han et al. (2007), (e) Yang et al. (2007), (f) case-Y1 (Yuan and Gao, 2010) and (g) case-Ga1 (Gao et al., 2011).

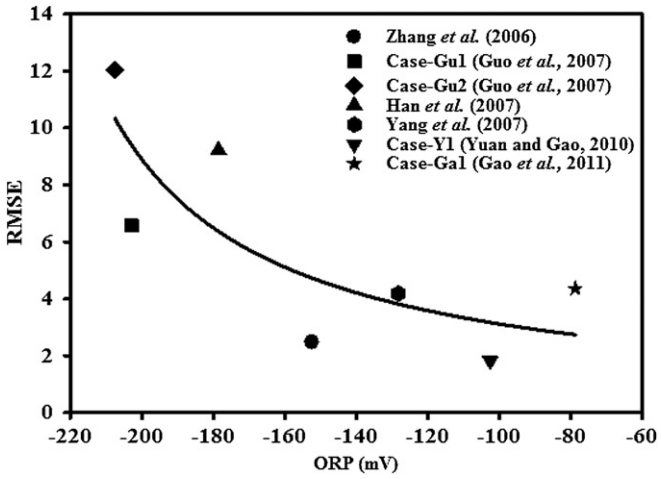

Fig. 2. Relationship between the final ORP values of biological denitrification and the RMSE values of simulation results.

overpotential. According to Tafel equation (Eq. (20)), the oxidation process and reduction process of a redox reaction induce an anodic current and a cathodic current transferring through the electrode interface separately, and the net value of both currents is correlated to the overpotential of redox couple (Petrii et al., 2007).

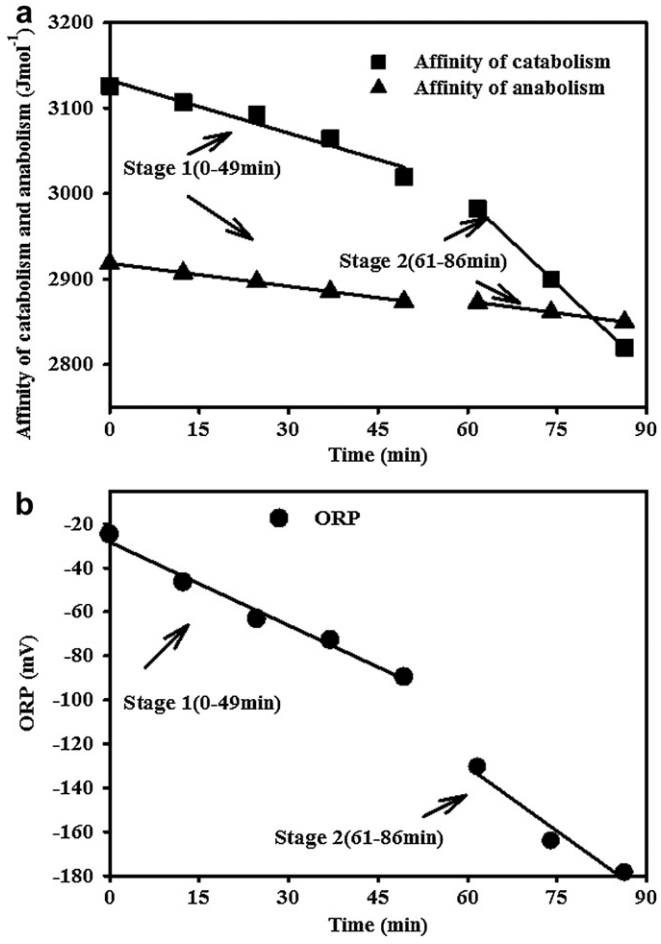

Fig. 3. Variation of (a) ORP and (b) affinities of catabolism and anabolism for Han et al. (2007).

$$\eta = a - b\log i \tag{20}$$

where "a" and "b" are Tafel constants, which are characteristic constants of the electrode system; and "i" is the current density that passes through the circuit of electrode ($A\,m^{-2}$).

Consequently, the magnitude of the net current passing through the electrode interface indirectly affects the sign of P_{EC} and P_{EA}.

Theoretically, P_{EC} and P_{EA} are not the function of the ORP or affinities of catabolism and anabolism, however, they can be related to the nature of biological denitrification processes (Demirel, 2002). A significant correlation ($r^2 = 0.80$) exists between the P_{EC} values and the molarities of electron transferred during catabolism of biological denitrification processes (M_e) as shown in Fig. 4. The molar concentration of electrons involved in the oxidation of carbon source to CO_2, H_2O, and NH_3 can be calculated by using the production of degree of reduction of carbon source (γ_{COD}), and molarity of carbon source consumed (C-mol L^{-1}). In addition, only a portion of electrons in carbon sources are used for catabolism, and therefore M_e is calculated based on the production of f_e and the molarity of electrons involved in the oxidation of carbon source. Fig. 4 shows that P_{EC} values decrease when the molarities of electron transferred increase; the results can be interpreted based on the theoretically linear relationship of the overpotential (η), and the affinity of the electrochemical reaction (A) shown in Eq. (21) (Gileadi, 1993).

$$\eta = E_{ne} - E_e = \frac{1}{n'F}A \tag{21}$$

When multiplied by the reciprocal of charge consumed per mole of reactants (n') and Faraday constant (F), affinity A is equal to the overpotential. Because P_{EC} is related to the coupling of affinity of catabolism and applied potential on ORP electrode, it is assumed to be proportional to the reciprocal of the number of electrons in the overall reaction (F is constant). This is further verified by the results shown in Fig. 4. As mentioned before that P_{EC} can be interpreted as the ORP change per unit affinity during catabolism, the ORP change per unit affinity during catabolism is inversely to M_e, or the affinity change per unit ORP is proportional to M_e. In this paper, the degree of reduction of the carbon sources reported in the cited literature close to the degree of reduction of biomass. Accordingly, the affinities of anabolism have a minor effect on ORP so that no

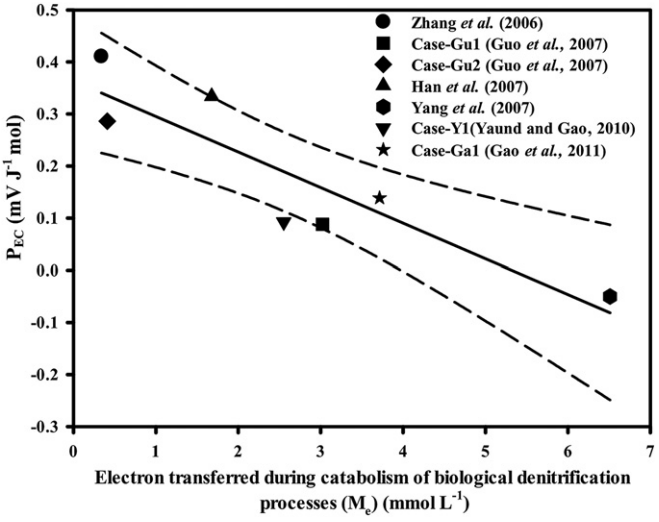

Fig. 4. Linear relationship between electron transferred during biological denitrification and the phenomenological parameter P_{EC}. Dashed lines indicate the 95% confidence interval of the linear regression line.

correlation between P_{EA} and the molarities of electron transferred during anabolism is found in this study.

3.3. The consistency of phenomenological parameters of MIRROR model No. 1

For testing the consistency of phenomenological parameter of MIRROR model No. 1, the data sets of case-Y2 and case-Y3 (Yuan and Gao, 2010) were simulated using the calibrated phenomenological parameters based on case-Y1 data set (Yuan and Gao, 2010). In addition, case-Ga2 data set (Gao et al., 2011) was simulated using the calibrated phenomenological parameters based on case-G1 data set (Gao et al., 2011). Calibrated phenomenological and kinetic parameters are shown in Table 5. The simulated and experimental data for the case-Y2, case-Y3 (Yuan and Gao, 2010) and case-Ga2 (Gao et al., 2011) are shown in Fig. 5 with the statistical evaluation results listed in Table 6. In all three cases, the trend of predictions can explain 98-99% of the variance in the observed ORP data ($R^2 = 0.98–0.99$). The hypothesis that distribution of residuals for regression lines (experimental data minus simulation data) must be normal distribution was tested by using Lilliefor's test. The results shown in Table 6 reveal that the residuals of simulation results using MIRROR model No. 1 can be considered as normally distributed.

Fig. 5(a) shows that the simulated results based on the case-Y2 (Yuan and Gao, 2010) data set fit perfectly the experimental data. This observation has also been confirmed by the values of RMSE (3.57) and R^2 (0.99). Although R^2 values of simulated case-Y3 data set (Yuan and Gao, 2010) are as high as 0.99; the simulated data set is systematic higher than the experimental data set, and the plot of simulated data is seen to be parallel to the plot of experimental data. In the study of Yuan and Gao (2010), DO concentrations were controlled at different levels during the aerobic stage. The remaining residual DO at the end of the aerobic stage affects the subsequent anoxic biological denitrification. It takes 5 min for case-Y1 and case-Y2 data sets (Yuan and Gao, 2010) and 10 min for the case-Y3 data set to deplete the oxygen concentration to 0 mg L^{-1} at the beginning of the anoxic stage. Moreover, the DO concentration in aerobic stage of case-Y1 data set (Yuan and Gao, 2010), i.e. 4.5 mg O_2 L^{-1}, was controlled at nearly similar level as for case-2 data set (3.5 mg O_2 L^{-1}) but not for case-3 data set (2.5 mg O_2 L^{-1}). Therefore, the phenomenological parameters of case-1 data set in Yuan and Gao's (2010) study is more suitable for simulating the ORP variation of their case-2 data set than simulating the ORP variation of their case-3 data set.

As shown in Fig. 5(c), the prediction results are noted to deviate from the experimental data at the end stage of the biological denitrification process for case-Ga2 data set (Gao et al., 2011). In the study of Gao et al. (2011), both flocculent activated sludge and aerobic granular sludge were used for investigate the influence of the seeding sludge on the nitrogen removal in the SBR system. These two types of seeding sludge have extremely different microbial characteristics; zoogloea exists in the flocculent activated sludge but not in the granular sludge. Furthermore, the simultaneous nitrification and denitrification are more likely to occur in the granular sludge than flocculent activated sludge. Because the diffusion of dissolved oxygen is more limited in the granular sludge than flocculent sludge, the layer structure of the former consists of aerobic and anoxic zones from the surface to the centre of granular structure. Hence, biological denitrification reaction can proceed

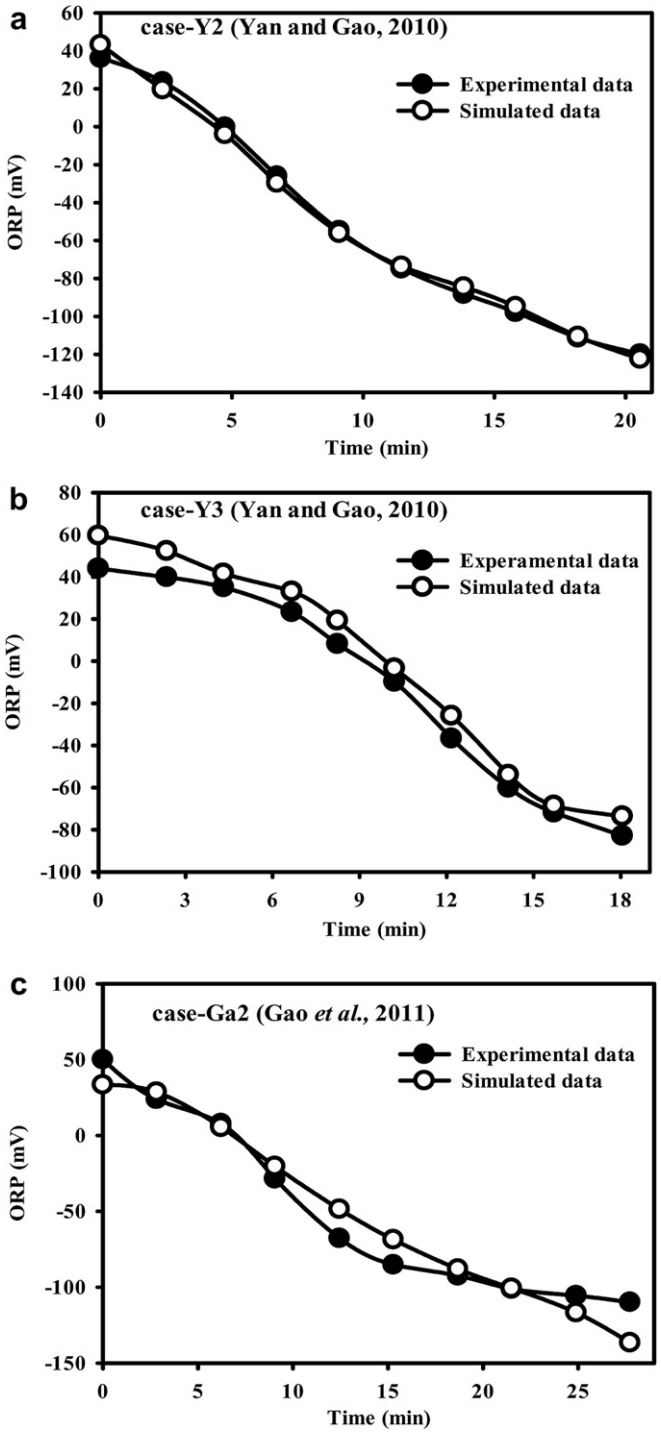

Fig. 5. The simulated and experimental ORP of case-Y2 and case-Y3 (Yuan and Gao, 2010) and case-Ga2 (Gao et al., 2011).

Table 5
Calibrated phenomenological and kinetics parameters of biological denitrification processes used for verifying the consistency of MIRROR model No. 1.

Literature	Case-Y2 (Yuan and Gao, 2010)	Case-Y3 (Yuan and Gao, 2010)	Case-Ga2 (Gao et al., 2011)
Carbon source	Glucose	Glucose	Glucose
f_e	0.64	0.64	0.64
f_s	0.36	0.36	0.36
$f_{NO_3^-}$	0.02	0.00	0.01
$f_{NO_2^-}$	0.98	1.00	0.99
K_1 (M)	4.76×10^{-7}	4.76×10^{-7}	4.76×10^{-7}
K_H (M atm^{-1})	2.94×10^{-2}	2.94×10^{-2}	2.94×10^{-2}
P_{EC} (mV mol J^{-1})	0.092	0.092	0.14
P_{EA} (mV mol J^{-1})	0.0067	0.0067	−0.0094
E_e (mV)	−417.38	−417.38	−530.24

Table 6
Statistical evaluation of the performances of the simulation results for case-Y2 and case-Y3 (Yuan and Gao, 2010) and case-Ga2 (Gao et al., 2011)

Literature	Lilliefor's statistics		R^2	RMSE
	D^*	$D_{0.025,10}$		
Case-Y2 (Yuan and Gao, 2010)	0.13	0.41	0.99	4.87
Case-Y3 (Yuan and Gao, 2010)	0.19	0.41	0.99	9.75
Case-G2 (Gao et al., 2011)	0.17	0.41	0.98	13.66

inside aerobic granules. Consequently, the mechanism of biological denitrification for these two types of seeding sludge may not be necessarily identical so that some deviation is observed between the simulated results and the case-Ga2 data set (Gao et al., 2011). In spite of these minor deficiencies, the simulated results are acceptable; therefore, the estimated phenomenological parameters are valid for describing the biological denitrification processes under similar conditions.

3.4. Application of MIRROR model No. 1 for predicting biological denitrification rate by ORP

According to Eqs. (2)–(4), all ORP and reaction rates of catabolism and anabolism are linearly related to affinities of catabolism and anabolism. Therefore, affinities of catabolism and anabolism can be used to relate ORP variations to reaction rates of catabolism and anabolism. Based on Eq. (3), affinities of catabolism and anabolism can be derived (Eq. (24)):

$$A_{BS}^{C} = \frac{J_C - P_{CA}A_{BS}^{A}}{P_{CC}} \tag{22}$$

Substituting Eq. (22) into Eq. (2) gives:

$$E_{ne} = E_e + \frac{P_{EC}}{P_{CC}}J_C - \left(\frac{P_{CA}}{P_{CC}} - P_{EA}\right)A_{BS}^{A} \tag{23}$$

Because the degradation rates in catabolism and anabolism may be different for various substrates, the net removal rate of a substrate can be represent as Eq. (24).

$$\frac{dS_{lim}}{dt} = S_{C,n}J_C + S_{A,n}J_A \tag{24}$$

where $S_{C,n}$ and $S_{A,n}$ are the stoichiometric coefficients of substrate of catabolism and anabolism, respectively.

When either catabolic or anabolic substrate is limiting, the linear relationship between catabolic substrate consumption and the microbial growth rate can be expressed as Eq. (25) by combining Eqs. (3) and (4) (Westerhoff et al., 1982):

$$J_C = \alpha(-J_A) + \beta \tag{25}$$

where α and β are constants.

If the substrate mainly used in catabolism is limited, replacing J_A in Eq. (24) by Eq. (25) will result in Eq. (26) to represent the reaction rate of the limited substrate:

$$\frac{dS_{lim}}{dt} = \left(S_{C,n} - \frac{S_{A,n}}{\alpha}\right)J_C + \frac{S_{A,n}\beta}{\alpha} \tag{26}$$

Eq. (26) can be rearranged as Eq. (27).

$$J_C = \frac{((dS_{lim}/dt) - (S_{A,n}\beta/\alpha))}{(S_{C,n} - (S_{A,n}/\alpha))} \tag{27}$$

Substituting Eq. (27) into Eq. (23) and rearranging as Eq. (28).

$$E_{ne} = E_e + \frac{P_{EC}}{P_{CC}\left(S_{C,n} - \frac{S_{A,n}}{\alpha}\right)}\frac{dS_{lim}}{dt} - \frac{P_{EC}}{P_{CC}}\left(\frac{S_{A,n}\beta/\alpha}{S_{C,n} - (S_{A,n}/\alpha)}\right) - \left(\frac{P_{CA}}{P_{CC}} + P_{EA}\right)A_{BS}^{A} \tag{28}$$

Unlike catabolism, the substrate used for anabolism is unlimited; therefore, the affinity of anabolism can be regarded as a constant, and Eq. (28) can be further simplified as Eq. (29)

$$E_{ne} = \chi\left(\frac{dS_{lim}}{dt}\right) + \delta \tag{29}$$

where χ and δ are constants.

According to Eq. (29), a linear relationship exists between the ORP under non-equilibrium conditions and the reaction rate when the biochemical system is under conditions in which the catabolic or anabolic substrate is growth limiting. For verifying the relationship, the experimental data reported by Almeida et al. (1995) on using a pure culture of *Pseudomonas fluorescens* for studying the kinetics of denitrification was used. In their study, an exponentially growing culture was suspended in a buffered anoxic acetate solution with pH values controlled at 6.6, 7.0, 7.4, and 7.8 using phosphate buffer. The system ORP was monitored once every 7 s. The nitrate reduction rate is predicted by using the Michaelis–Menten equation, and Eq. (29) is verified by the plot of nitrate reduction rate vs. ORP for different pH values, as shown in Fig. 6. The linear relationships between ORP and denitrification rate suggests that ORP increases linearly with the increase of denitrification rate within the ORP interval in question (−110 to 110 mV). The denitrification rate can be estimated by using ORP as a surrogate indicator so that a continuous nitrogen removal in the biological denitrification processes can be maintained.

In addition to Almeida et al. (1995), Lie and Welander (1994) also considered the effect of ORP on biological denitrification rate in batch operations. In their study, the ORP in the batch reactors was maintained at preset levels by regulating the aeration for investigating the influence of low concentrations of dissolved oxygen on the denitrification activity of activated sludge. In their plots of ORP vs. biological denitrification rate, a linear relationship was observed. The slope of the straight line differed considerably in magnitude with respect to types of sludge samples and carbon sources. However, the ORP was observed to increase linearly with decreasing denitrification rate that differs from the results reported by Almeida et al. (1995). In the study of Lie and Welander (1994), ORP of batch cultures were controlled by aeration; therefore, dissolved oxygen will affect the measurement of ORP. Although the denitrifying activity immediately began and the concentration of nitrite and nitrate continuously decrease when the conditions of the sequencing batch reactor change from aerobic to anoxic period, the residual dissolved oxygen is maintained at 1 mg L^{-1} for additional 10 min. Because electroactive species, e.g. DO, will directly exchange electrons with electrode by adsorption, the presence of dissolved oxygen affects electron transfer between the electrode surface and the bulk solution (Peiffer et al., 1992).

Besides, the linear relationship between ORP and reaction rate under substrate limited conditions can be used to enhance the technology using ORP as a reaction rate indicator. Spérandio and Queinnec (2004) developed a software sensor, based on ORP and DO measurements, for simultaneously estimating nitrogen concentration in wastewater, nitrification rate, and denitrification rate. Signal dynamics of ORP is used for identification of the end of denitrification reaction; the ORP profile indicating zero

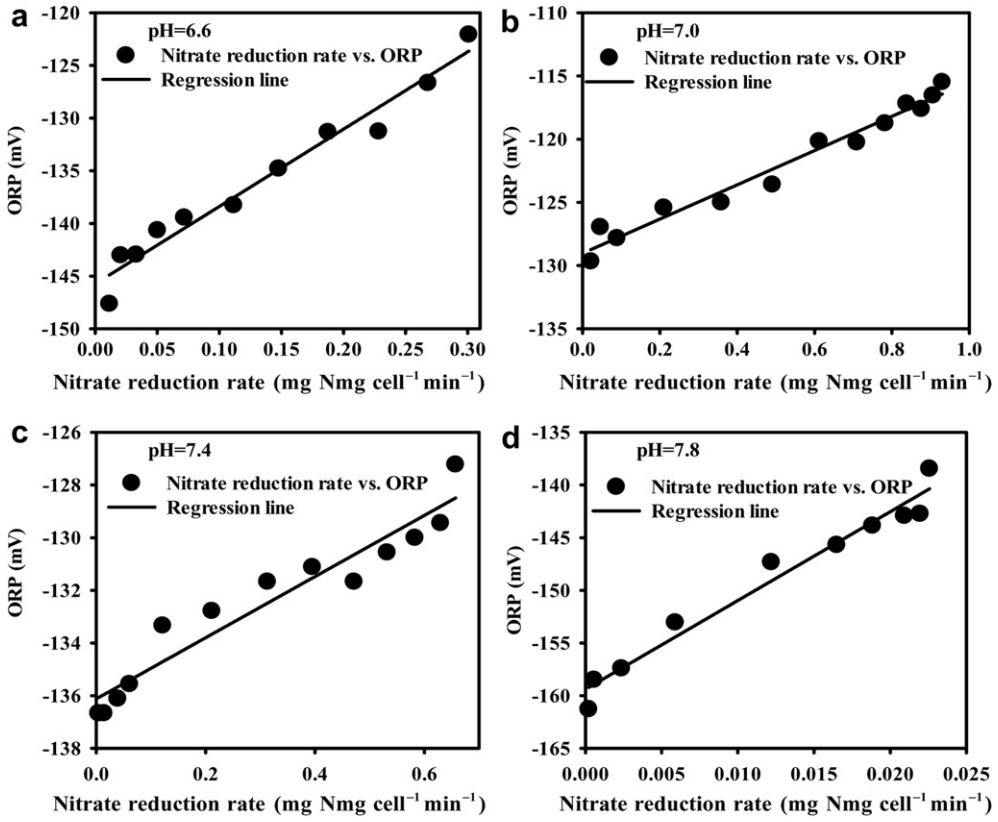

Fig. 6. Linear relationship between the reaction rate and ORP value of biological denitrification.

denitrification activity is reached when a bending point is observed (Tanwar et al., 2008). However, the bending point disappears when biological denitrification processes are under substrate limited conditions. If the denitrification rate under conditions of limiting substrate can be estimated by using the linear relationship between ORP and reaction rate, the software sensor developed by Spérandio and Queinnec (2004) will be applied to a wider scope of experimental conditions.

4. Conclusions

The MIRROR model No. 1, using linear non-equilibrium thermodynamics, was implemented to simulate the biological denitrification processes and the variations of ORP during biological denitrification processes were characterized by affinities of catabolism and anabolism. Results of modeling efficiency and model discrimination analyses show that MIRROR model No. 1 is superior to the modified Nernst equation for simulating ORP variations of a biological denitrification system. Moreover, the ORP variations of biological denitrification processes are better fitted by the results of MIRROR model No. 1 than the modified Nernst equation.

During catabolism of biological denitrification processes, the affinity change per unit ORP is not a constant for different experimental conditions, but proportional to molarities of electron transferred. The implementation of MIRROR model No. 1 will enable one to extract more information from the redox measurement of biological processes.

Acknowledgements

We would like to thank the National Science Council of Taiwan, ROC for financial support of this research (NSC 92-2622-E-009-021-CC3).

References

Almeida, J.S., Reis, M.A., Carrondo, M.J., 1995. Competition between nitrate and nitrite reduction in denitrification by Pseudomonas fluorescens. Biotechnology and Bioengineering 46, 476–484.
Balakireva, L.M., Kantere, V.M., Rabotnova, I.L., 1974. The redox potential in microbiological media. Biotechnology and Bioengineering Symposium 4, 769–780.
Box, G.E.P., Hill, W.J., 1967. Discrimination among mechanistic models. Technometrics 9, 57–71.
Chang, C.-N., Cheng, H.-B., Chao, A.C., 2004. Applying the Nernst equation to simulate redox potential variations for biological nitrification and denitrification processes. Environmental Science & Technology 38, 1807–1812.
Chapra, S.C., 1997. pH Modeling, Surface Water-quality Modeling. McGraw-Hill, New York. 683–691.
Cheng, H.-B., Kumar, M., Lin, J.-G., 2007. Development of linear irreversible thermodynamic model for oxidation reduction potential in environmental microbial system. Biophysical Journal 93, 787–794.
Confalonieri, R., Bregaglio, S., Bocchi, S., Acutis, M., 2010. An integrated procedure to evaluate hydrological models. Hydrological Processes 24, 2762–2770.
Dallal, G.E., Leland, W., 1986. An analytic approximation to the distribution of Lilliefors's test statistic for normality. The American Statistician 40, 294–296.
Demirel, Y., 2002. Linear Nonequilibrium Thermodynamics, Nonequilibrium Thermodynamics: Transport and Rate Processes in Physical and Biological Systems. Elsevier science, New York. 59–83.
Demirel, Y., Sandler, S.I., 2002. Thermodynamics and bioenergetics. Biophysical Chemistry 97, 87–111.
Demirel, Y., Sandler, S.I., 2004. Nonequilibrium thermodynamics in engineering and science. The Journal of Physical Chemistry B 108, 31–43.
Duboc, P., Schill, N., Menoud, L., van Gulik, W., von Stockar, U., 1995. Measurements of sulfur, phosphorus and other ions in microbial biomass: influence on correct determination of elemental composition and degree of reduction. Journal of Biotechnology 43, 145–158.
Gao, D., Yuan, X., Liang, H., Wu, W.M., 2011. Comparison of biological removal via nitrite with real-time control using aerobic granular sludge and flocculent activated sludge. Applied Microbiology and Biotechnology 89, 1645–1652.
Gileadi, E., 1993. Electrode Kinetics for Chemists, Chemical Engineers, and Materials Scientists. Wiley-VCH, New York.
Guo, J., Yang, Q., Peng, Y., Yang, A., Wang, S., 2007. Biological nitrogen removal with real-time control using step-feed SBR technology. Enzyme and Microbial Technology 40, 1564–1569.
Han, Z., Wu, W., Chen, Y., Zhu, J., 2007. Characteristics of a twice-fed sequencing batch reactor treating swine wastewater under control of aeration intensity. Journal of Environmental Science and Health, Part A 42, 361–370.

Han, Z.Y., Wu, W.X., Zhu, J., Chen, Y.X., 2008. Oxidization-reduction potential and pH for optimization of nitrogen removal in a twice-fed sequencing batch reactor treating pig slurry. Biosystems Engineering 99, 273–281.
Heijnen, J.J., 1999. Balance of degree of reduction, atomic degrees of reduction, and the COD balance. In: Flickinger, M.C., Drew, S.W. (Eds.), Encyclopedia of Bioprocess Technology: Fermentation, Biocatalysis, and Bioseparation. Wiley, John & Sons, New York, pp. 281–282.
Kjaergaard, L., 1977. The redox potential: its use and control in biotechnology. Advances in Biochemical Engineering 7, 131–150.
Lie, E., Welander, T., 1994. Influence of dissolved oxygen and oxidation-reduction potential on the denitrification rate of activated sludge. Water Science and Technology 30, 91–100.
Mayer, D.G., Butler, D.G., 1993. Statistical validation. Ecological Modelling 68, 21–32.
Mayer, D.G., Stuart, M.A., Swain, A.J., 1994. Regression of real-world data on model output: an appropriate overall test of validity. Agricultural Systems 45, 93–104.
Nagpal, S., Chuichulcherm, S., Livingston, A., Peeva, L., 2000. Ethanol utilization by sulfate-reducing bacteria: an experimental and modeling study. Biotechnology and Bioengineering 70, 533–543.
Nielsen, J., 1997. Metabolic control analysis of biochemical pathways based on a thermokinetic description of reaction rates. Biochemical Journal 321, 133–138.
Paul, E., Plisson-Saune, S., Mauret, M., Cantet, J., 1998. Process state evaluation of alternating oxic–anoxic activated sludge using ORP, pH and DO. Water Science and Technology 38, 299–306.
Peiffer, S., Klemm, O., Pecher, K., Hollerung, R., 1992. Redox measurement in aqueous solutions – a theoretical approach to data interpretation, based on electrode kinetics. Journal of Contaminant Hydrology 10, 1–18.
Petrii, O.A., Nazmutdinov, R.R., Bronshtein, M.D., Tsirlina, G.A., 2007. Life of the Tafel equation: current understanding and prospects for the second century. Electrochimica Acta 52, 3493–3504.
Plisson-Saune, S., Capdeville, B., Mauret, M., Deguin, A., Baptiste, P., 1996. Real-time control of nitrogen removal using three ORP bending-points: signification, control strategy and results. Water Science and Technology 33, 275–280.
Rittmann, B.E., McCarty, P.L., 2001. Metabolism, Environmental Biotechnology: Principles and Applications. McGraw-Hill, New York. 55–79.
Rothschild, K.J., Ellias, S.A., Essig, A., Stanley, H.E., 1980. Nonequilibrium linear behavior of biological systems. Existence of enzyme-mediated multidimensional inflection points. Biophysical Journal 30, 209–230.
Rottenberg, H., 1973. The thermodynamic description of enzyme-catalyzed reactions. The linear relation between the reaction rate and the affinity. Biophysical Journal 13, 503–511.
Spérandio, M., Queinnec, I., 2004. Online estimation of wastewater nitrifiable nitrogen, nitrification and denitrifiation rates, using ORP and DO dynamics. Water Science and Technology 49, 31–38.
Stumm, W., 1966. Redox potential as an environmental parameter: conceptual significance and operational limitation. Third International Conference on Water Pollution Research. Water Pollution Control Federation, Germany, pp. 283–308.
Stumm, W., Morgan, J.J., 1996. Oxidation and Reduction; Equilibria and Microbial Mediation, Aquatic Chemistry: Chemical Equilibria and Rates in Natural Waters. John Wiley & Sons, Inc., New York. 425–470.
Tanwar, P., Nandy, T., Ukey, P., Manekar, P., 2008. Correlating on-line monitoring parameters, pH, DO and ORP with nutrient removal in an intermittent cyclic process bioreactor system. Bioresource Technology 99, 7630–7635.
Tedeschi, L.O., 2006. Assessment of the adequacy of mathematical models. Agricultural Systems 89, 225–247.
Van Boekel, M.A.J.S., 2008. Kinetic modeling of food quality: a critical review. Comprehensive Reviews in Food Science and Food Safety 7, 144–158.
van der Meer, R., Westerhoff, H.V., Van Dam, K., 1980. Linear relation between rate and thermodynamic force in enzyme-catalyzed reactions. Bioehimica et Biophysica Acta 591, 488–493.
Westerhoff, H.V., Hellingwerf, K.J., Dam, K.V., 1983. Thermodynamic efficiency of microbial growth is low but optimal for maximal growth rate. Proceedings of the National Academy of Sciences USA 80, 305–309.
Westerhoff, H.V., Lolkema, J.S., Otto, R., Hellingwerf, K.J., 1982. Thermodynamics of growth. Non-equilibrium thermodynamics of bacterial growth. The phenomenological and the mosaic approach. Bioehimica et Biophysica Acta 683, 181–220.
Xiao, J., VanBriesen, J.M., 2008. Expanded thermodynamic true yield prediction model: adjustments and limitations. Biodegradation 19, 99–127.
Yang, Q., Wang, S., Yang, A., Guo, J., Bo, F., 2007. Advanced nitrogen removal using pilot-scale SBR with intelligent control system built on three layer network. Frontiers of Environmental Science & Engineering in China 1, 33–38.
Yuan, X., Gao, D., 2010. Effect of dissolved oxygen on nitrogen removal and process control in aerobic granular sludge reactor. Journal of Hazardous Materials 178, 1041–1045.
Zhang, Z., Zhu, J., King, J., Li, W., 2006. A two-step fed SBR for treating swine manure. Process Biochemistry 41, 892–900.

Nomenclature

γ_{COD}: the degree of reduction of an organic compound
χ: the slope
δ: the intercept
η: overpotential of redox couple (V)
A^C_{BS}: the affinity of catabolism (C) occurring in bulk solution (BS) (J mol^{-1})
A^A_{BS}: the affinity of anabolism (A) occurring in bulk solution (BS) (J mol^{-1})
CDF: the normal cumulative distribution function with mean and standard deviation equal to the mean and standard deviation of the sample
E_{ne}: electrode potentials under non-equilibrium conditions (V)
E_e: electrode potentials under equilibrium conditions (V)
EF: the modeling efficiency
f_e: the fraction of total electron used for energy production
f_s: the fraction of total electrons used for biomass synthesis
$f_{NO_3^-}$: fractions of nitrate finally transferring to nitrite
$f_{NO_2^-}$: fractions of nitrate finally transferring to nitrogen gas
F: Faraday constant (96,500 C mol^{-1})
F-test$_{s1,i0}$: the simultaneous *F* test for slope = 1 and intercept = 0
ΔG^0_C: the change in standard Gibbs free energy of catabolism (J mol^{-1})
ΔG^0_A: the change in standard Gibbs free energy ofa nabolism (J mol^{-1})
i: the current density that passes through the circuit of electrode (A m^{-2})
J_C: the reaction rates of catabolism (C-mol g^{-1} h^{-1})
J_A: the reaction rates of anabolism (C-mol g^{-1} h^{-1})
K_1: the first dissociation constant of carbonic acid
M_e: the molarities of electron transferred during catabolism of biological denitrification processes (M)
n': charge consumed per mole of reactants during electrode processes
P_{EC}, P_{EA}, P_{CC}, P_{CA}, P_{AC}, P_{AA}: phenomenological parameters
R: gas constant (8.314 J mol^{-1} K^{-1})
R^2: the adjusted coefficient of determination
RMSE: the root mean square error
RSS: the residual sums of squares
S: the stoichiometric coefficient (positive for products and negative for reactants)
SCDF: the estimated empirical cumulative distribution function based on the sample
$S_{C,n}$: the stoichiometric coefficients of substrate of catabolism
$S_{A,n}$: the stoichiometric coefficients of substrate of anabolism
T: absolute temperature (K)
X: the molar concentration of redox species (M)